Topics in Catalysis (2018) 61:1672–1683
https://doi.org/10.1007/s11244-018-1022-2

ORIGINAL PAPER

Dynamics and Selectivity of N_2O Formation/Reduction During Regeneration Phase of Pt-Based Catalysts

Lidia Castoldi[1] · Roberto Matarrese[1] · Chuncheng Liu[1] · Sara Morandi[2] · Luca Lietti[1]

Published online: 26 July 2018

Abstract
The formation of N_2O has been studied by means of isothermal lean-rich experiments at 150, 180 and 250 °C over Pt–Ba/Al_2O_3 and Pt/Al_2O_3 catalysts with H_2 and/or C_3H_6 as reductants. This allows to provide further insights on the mechanistic aspects of N_2O formation and on the influence of the storage component. Both gas phase analysis and surface species studies by operando FT-IR spectroscopy were performed. N_2O evolution is observed at both lean-to-rich (primary N_2O) and rich-to-lean (secondary N_2O) transitions. The production of both primary and secondary N_2O decreases by increasing the temperature. The presence of Ba markedly decreases secondary N_2O formation. FT-IR analysis shows the presence of adsorbed ammonia at the end of the rich phase only for Pt/Al_2O_3 catalyst. These results suggest that: (i) primary N_2O is formed when undissociated NO in the gas phase and partially reduced metal sites are present; (ii) secondary N_2O originates from reaction between adsorbed NH_3 and residual NO_x at the beginning of the lean phase. Moreover, N_2O reduction was studied performing temperature programming temperature experiments with H_2, NH_3 and C_3H_6 as reducing agents. The reduction is completely selective to nitrogen and occurs at temperature higher than 250 °C in the case of Pt–Ba/Al_2O_3 catalyst, while lower temperatures are detected for Pt/Al_2O_3 catalyst. The reactivity order of the reductants is the same for the two catalysts, being hydrogen the more efficient and propylene the less one. Having H_2 a high reactivity in the reduction of N_2O, it could react with N_2O when the regeneration front is developing. Moreover, also ammonia present downstream to the H_2 front could react with N_2O, even if the reaction with stored NO_x seems more efficient.

Keywords N_2O reduction · N_2O formation · Lean NO_x Trap · NO_x storage reduction · Pt–Ba/Al_2O_3 · Pt

1 Introduction

After Euro 6 emission standards coming into force for light duty vehicle from 2014, the car manufactures of diesel-engine and light-duty direct-injection (DI) gasoline-engine in Europe are facing severe challenges in terms of NO_x emissions reduction [1, 2].

The NO_x storage and reduction (NSR) catalysts, also referred as lean NO_x traps (LNTs), represent a viable solution for the NO_x removal from the exhaust gas of lean gasoline and diesel powered engines. The catalysts contain three fundamental components: a high surface area support (like γ-Al_2O_3), NO_x storage materials (typically Ba, K) and precious metals (such as Pt, Rh, Pd). Promoters and additives like Ce, Zr may be also included to increase thermal stability and add OSC (Oxygen Storage Capacity) functionality. The removal of nitrogen oxides is accomplished under transient operation; during long lean periods (60–90 s) NO_x are adsorbed over the storage component in form of nitrites/nitrates [3]; then, upon rich spikes (1–3 s) of the engine, the surface is regenerated. The reductants needed for the catalyst regeneration may also be originated from direct fuel injection in the exhausts, or from an upstream fuel reformer to give a reducing gas containing mainly CO and H_2. Catalyst regeneration mainly leads to N_2, however other byproducts like N_2O, NH_3 or unconverted NO may also be detected.

Nitrous oxide is highly undesired byproduct due to its high global warming potential, ~300 times higher than CO_2 [4]. N_2O emissions during operation of LNT catalyst are typically

✉ Lidia Castoldi
lidia.castoldi@polimi.it

[1] Dipartimento di Energia, Laboratory of Catalysis and Catalytic Processes, Politecnico di Milano, Via La Masa, 34, 20156 Milan, Italy

[2] Dipartimento di Chimica and NIS, Inter-Departmental Center, Università di Torino, Via Pietro Giuria 7, 10125 Turin, Italy

observed during both the lean-to-rich and rich-to-lean phase switching (primary and secondary N_2O, respectively) when using H_2, CO or C_3H_6 as reductant [5–8]. In the case of primary N_2O formation, it was suggested that the extent of N_2O formation depends on the reducibility of the noble metal (PGM) sites [9]. Depending on the efficiency of the reductant in the oxygen removal from the PGM sites, different amounts of N_2O will be detected, i.e. the lower is the reduction capacity, the higher is the N_2O production. Different factors affect the N_2O formation when the catalytic system is switched from rich to lean (secondary emissions): in this case the residual reduced species like NH_x (x = 1–3), isocyanate or hydrocarbons could react with gaseous NO/O_2 to give N_2O.

N_2O emission control is an important issue nowadays for any emission technology, and several ways have been proposed to reduce them. The catalytic decomposition over a catalyst placed downstream the LNT brick might be a viable solution to decompose/reduce N_2O after its formation (deN_2O reaction). A variety of catalytic systems has been proposed and tested for this purpose [10], including metal oxides [11–13] and ion-exchange zeolites [14, 15]. Furthermore, some authors report high activity for catalytic systems based on cobalt, copper, iron, and especially noble metals [16, 17].

In this work, the focus is on the pathways involved in the formation of N_2O during the cyclic operations of a typical LNT catalysts. For these purposes, lean/rich cycles under isothermal conditions have been carried out over two homemade model catalysts with and without the storage component, i.e. Pt-Ba/Al_2O_3 (1/20/100 w/w) and Pt/Al_2O_3 (1/100 w/w). To get more insights on the reaction pathways occurring in the evolution of nitrous oxide during lean/rich cycles, the decomposition/reduction of N_2O has also been investigated over the same catalytic systems. Accordingly, temperature-programmed reduction (TPR) experiments have been performed to investigate the N_2O decomposition and reduction with different reductants.

In these experiments hydrogen has been employed as reducing agent, being this species the most effective (and idealized) NO_x reductant thanks to its simple chemistry and effectiveness [18–22]. For comparison purposes, C_3H_6 has also been used as more representative reducing species present in the exhausts.

Flow-reactor experiments and *operando* FT-IR spectroscopy are used as complementary tools to combine the catalyst surface species with gas-phase data.

2 Materials and Methods

Homemade Pt/γ-Al_2O_3 (1/100 w/w) and Pt–Ba/γ-Al_2O_3 (1/20/100 w/w) catalysts have been prepared by standard incipient wetness impregnation of commercial γ-alumina support. The obtained catalysts have a specific surface area of 182 and 133 m^2/g (BET method) and pore volume 0.94 and 0.68 cm^3/g (cumulative adsorption BJH method), respectively.

All experiments have been performed in a quartz flow-microreactor of 7 mm I.D. In each run 60 mg of catalyst (70–100 μm) and total flow of 100 Ncc/min have been used. A complete quantitative detection of the reaction products has been obtained through a combined use of MS (Thermostar 200, Pfeiffer Vacuum), UV–Vis NO_x and NH_3 analyzer (LIMAS 11HW, ABB), MultiGas FT-IR (mod. 2030, MKS) and a micro-gas chromatograph (3000A, Agilent), as detailed in previous works [23, 24].

The formation of N_2O has been studied by means of lean-rich cycles in the range 150–250 °C. These experiments consist in alternating rectangular step feeds of NO (1000 ppm) + 3% v/v O_2 in flowing He (lean phase), with rich phases (H_2 2000 ppm or C_3H_6 450 ppm + 2.5% v/v H_2O in He), until reproducible cycles are obtained. Catalyst conditioning involves the modification of the active storage Ba sites from the initial carbonate form (as loaded in the reactor) to the actual form under reaction conditions, i.e. carbonate, hydroxide, oxide [22, 25]. The relative amounts of the various Ba species depend on the gas phase composition, i.e. nature of the reducing agent, presence/absence of CO_2 and water. The reactivity of the different Ba species in the NO_x storage-reduction has been analyzed elsewhere [26].

The evolution of the surface species at 150 °C has been also analyzed by FT-IR spectroscopy performed under *operando* conditions with an IR reactor cell (ISRI Infrared Reactor, Granger, IN, USA) by using the catalysts in form of self-supported wafers (13 mg, diameter = 13 mm). The IR spectra were collected with a FT-IR Vertex 70 (Bruker, Billerica, MA, USA) spectrometer with 4 cm^{-1} spectral resolution and accumulation of 64 scans using a mercury–cadmium–telluride (MCT) detector. The NO_x storage (NO (1000 ppm) + O_2 (3% v/v) in He) and reduction (H_2 (2000 ppm) in He) were performed under a flow of 50 Ncc/min. As in the case of the catalytic tests, the catalysts have been pre-conditioned with several adsorption/reduction cycles. The spectra are reported as difference spectra in the figures. The background spectrum is always that obtained after the conditioning treatment.

In the choice of the operating conditions, the length of the lean and the rich phases is not representative of real operating conditions but it has been exaggerated to better enlighten the processes occurring at the surface. Besides, the reductant concentration has been kept low to avoid excessive temperature effects during the switches.

Finally, the reactivity of N_2O (500 ppm in Ar) was investigated by temperature-programmed reduction (TPR) experiments in the temperature range 40–500 °C (heating rate 10 °C/min) by using H_2 (2000 ppm in He) and C_3H_6 (1000 ppm in He) as reductants. Since ammonia is

also formed during lean-rich experiments, the reactivity of this species (1000 ppm in He) has also been investigated. Experiments have been performed in the presence of CO_2 (1000 ppm) and H_2O (2.5% v/v).

3 Results and Discussion

3.1 N_2O Formation

The results of isothermal lean-rich experiments carried out over Pt–Ba/Al_2O_3 catalyst with H_2 as reductant (gas-phase and surface analysis) carried out at low temperature (150 °C) are shown in Figs. 1 and 2, respectively. Note that the complete experiments comprehend many lean-rich cycles up to

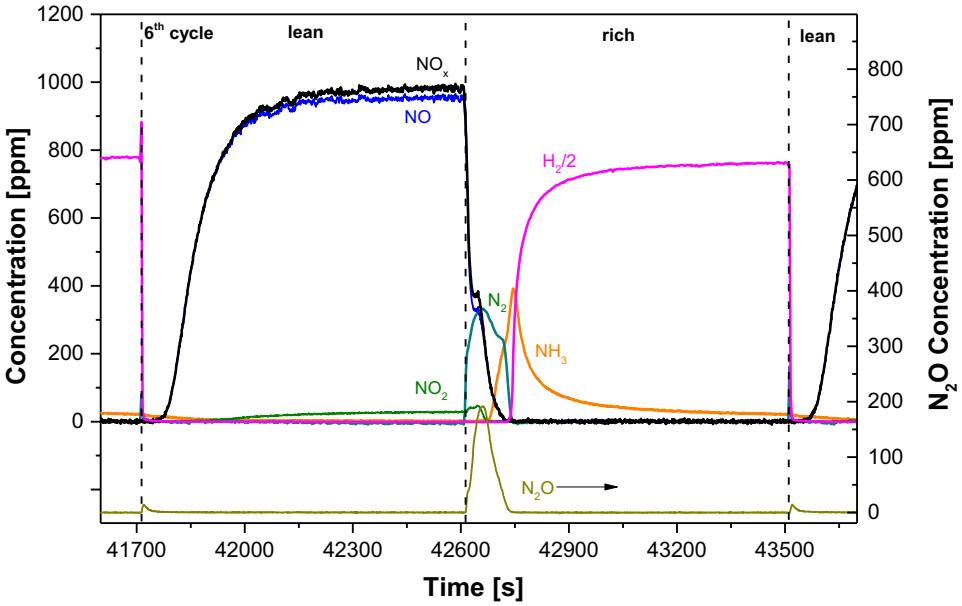

Fig. 1 Lean-rich cycles with H_2 at 150 °C over Pt–Ba/Al_2O_3 catalyst. Lean conditions: NO (1000 ppm) + 3% v/v O_2 in He; rich conditions: H_2 2000 ppm in He

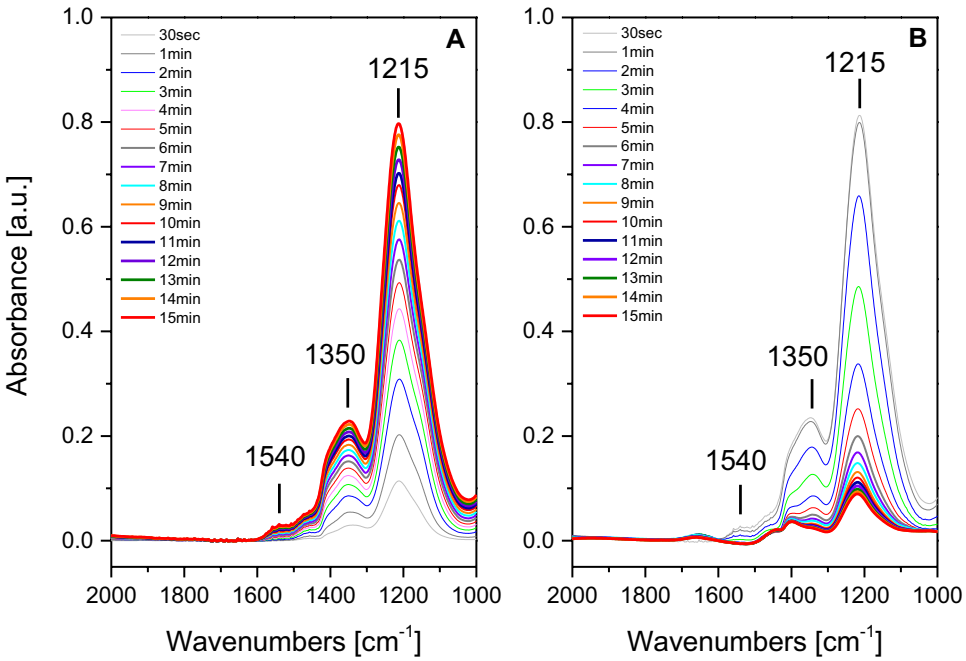

Fig. 2 *Operando* FTIR spectra at 150 °C over Pt–Ba/Al_2O_3 catalyst. **a** Lean phase NO (1000 ppm) + 3% v/v O_2 in He; **b** rich phase H_2 2000 ppm in He

reaching the steady-state conditions, while in the Figure the most representative one is reported for each catalyst.

Upon NO addition (lean phase, Fig. 1), the NO concentration increases monotonically with time showing a non-negligible dead time, while NO_2 is observed in negligible amounts due to the low temperature (the NO to NO_2 oxidation is not relevant). No other species have been observed, if one excludes a minor N_2O peak at the rich-to-lean transition.

Upon the subsequent lean-rich switch, the NO_x concentration decreases with a tail and instantaneous production of N_2 is observed and of NH_3 later on. Significant amounts of N_2O are also detected while the NO concentration is decreasing.

The surface FT-IR analysis of the lean phase is reported in Fig. 2a and shows the formation of mainly ionic nitrites on Ba sites (bands at 1350 cm^{-1}, $\nu_{sym}.(NO_2)$ and at 1215 cm^{-1}, $\nu_{asym}.(NO_2)$). Upon increasing the exposure time, a small band at 1540 cm^{-1} is also observed, which is related to bidentate nitrates [3]. On the other hand, FT-IR spectra recorded during the reduction (Fig. 2b) show the gradual consumption of nitrites, upon H_2 exposure, without the formation of other surface species. Only minor amounts of nitrites are still present at the end of the rich phase.

On Pt/Al_2O_3, upon the admission of NO during the lean phase a very small dead-time in the NO breakthrough is observed at the reactor outlet (Fig. 3); small amount of NO_2 are observed due to the higher oxidation activity of the Ba-free catalyst. A significant N_2O peak has also been observed at the rich-to-lean transition.

Upon the lean-rich switch, a tail is observed in the NO_x concentration; simultaneously minor amounts of N_2 and NH_3 are detected at the reactor outlet. Non-negligible amounts of N_2O are also detected, although in smaller amounts than those observed in the case of the $Pt–Ba/Al_2O_3$ catalyst.

Surface analysis obtained during the lean phase (Fig. 4a) shows the main formation of nitrites on Al_2O_3 sites (both ionic, $\nu_{asym}.(NO_2)$ and $\nu_{sym}.(NO_2)$ modes at 1230 and 1314 cm^{-1}, respectively, and linear, ν(N–O) and ν(N=O) modes at 1079 and 1548 cm^{-1}, respectively). Minor amounts of bidentate nitrates (ν(N=O) modes at 1610 and 1470 cm^{-1}) are also observed. Upon H_2 admission (Fig. 4b), the progressive consumption of nitrites is observed. Minor amounts of nitrites are still present at the end of the rich phase. However, as opposed to $Pt–Ba/Al_2O_3$, over the Pt/Al_2O_3 catalyst the reduction of nitrites is also accompanied by the appearance of new bands, i.e. at 1256 and 1620 cm^{-1}. According to the literature, these bands can be related to coordinated ammonia species on surface Lewis sites (symmetric deformation and asymmetric deformation, respectively), while the lower intensities bands at 1397, 1486 and 1688 cm^{-1} can be associated to surface ammonium ions, whose formation enlightens the presence of Brønsted acid sites of alumina [27–29]. Moreover, this assignment is in line with results from a dedicated experiment where the ammonia interaction (i.e. 150 ppm in He) with Pt/Al_2O_3 at 150 °C was tested (see dotted line in Fig. 4b).

Lean-rich cycles at 150 °C have also been carried out over $Pt–Ba/Al_2O_3$ catalyst using propylene as reductant in the presence of water. A representative cycle in these conditions is reported in Fig. 5. The reactivity of the catalyst when propylene is used as reducing agent is very poor: the dead time for NO breakthrough is very small, near 10 s, much shorter than in the case of H_2 as reductant. Minor amounts of NO_2 are also observed at the reactor outlet, together with CO_2 at the beginning of the lean phase due to the decomposition of Ba-carbonates upon formation of the adsorbed NO_x species [25, 30]. The presence of surface

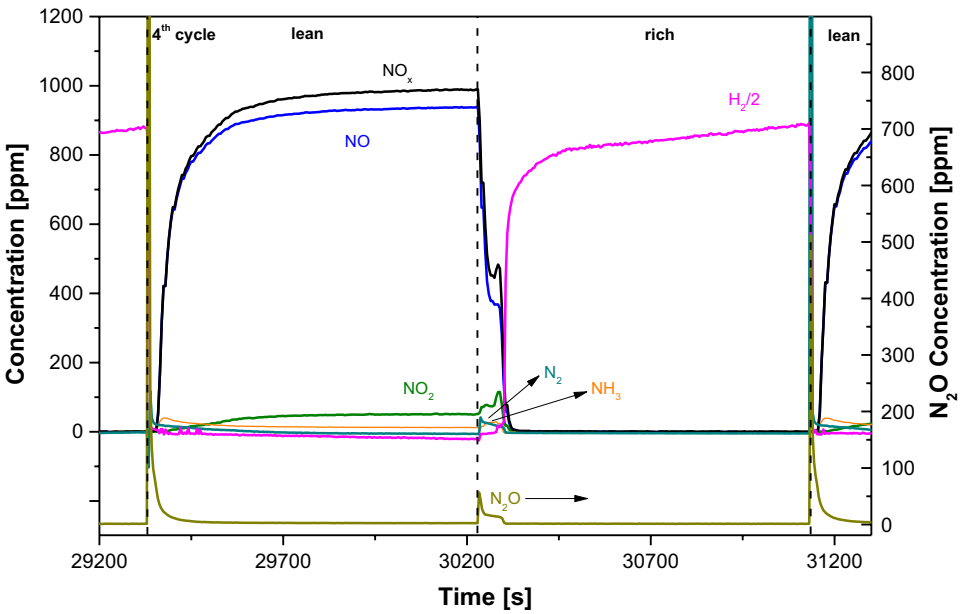

Fig. 3 Lean-rich cycles at 150 °C over Pt/Al_2O_3 catalyst. Lean conditions: NO (1000 ppm) + 3% v/v O_2 in He; rich conditions: H_2 2000 ppm in He

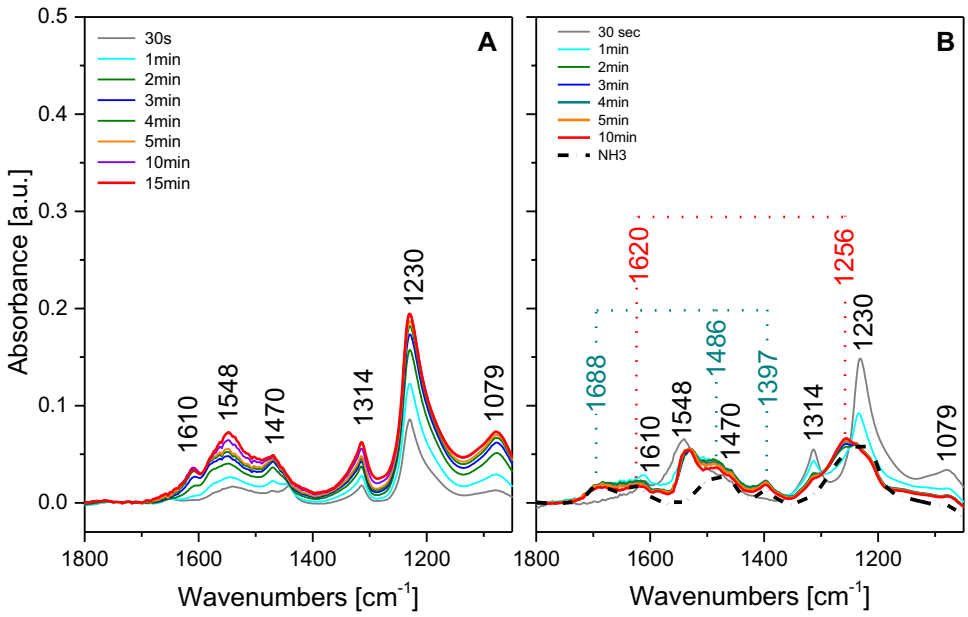

Fig. 4 *Operando* FTIR spectra at 150 °C over Pt/Al_2O_3 catalyst. **a** Lean phase NO (1000 ppm) + 3% v/v O_2 in He; **b** rich phase H_2 2000 ppm in He; dotted spectrum: 30 min. NH_3 adsorption (150 ppm in He at 150 °C)

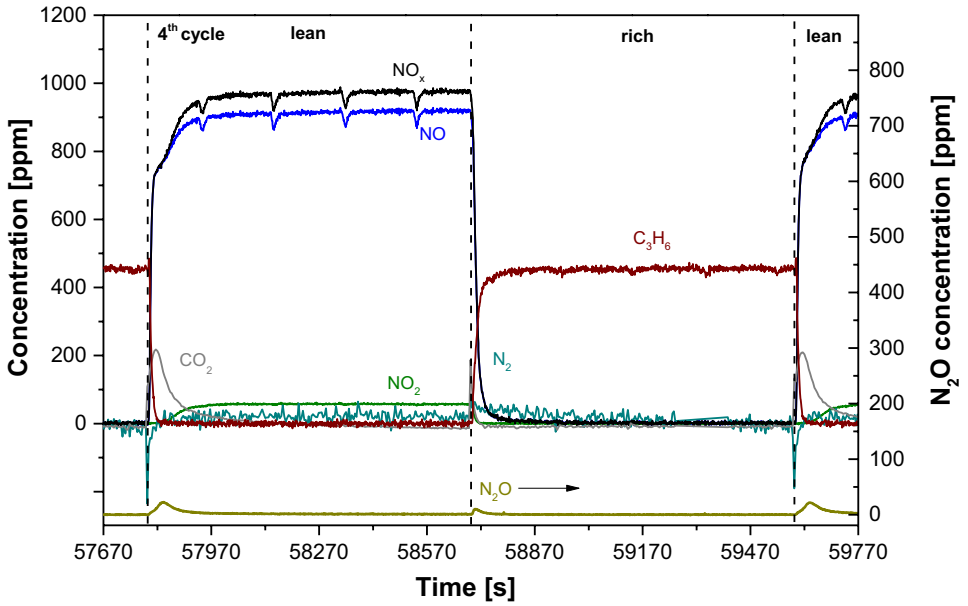

Fig. 5 Lean-rich cycles with C_3H_6 at 250 °C over Pt–Ba/Al_2O_3 catalyst. Lean conditions: NO (1000 ppm) + 3% v/v O_2 in He; rich conditions: C_3H_6 450 ppm + 2.5% v/v H_2O in He

carbonates is expected when propylene is used as reductant: the reduction process produces CO_2 that is adsorbed as carbonates. At the beginning of the lean phase, N_2O evolution is also observed.

When switching rich, NO_x concentration decreases with a small tail, and negligible amount of N_2 are observed together with a small peak of N_2O. Propylene rapidly reaches the inlet steady state concentration, due to the limited amounts of NO_x stored on the surface. This is likely related to both the presence of surface carbonates (that decrease the NO_x storage) and to the low activity of propylene as reductant, which is not able to fully reduce surface NO_x at such low temperature.

Lean-rich cycles have been performed also at higher temperature, e.g. 180 and 250 °C over Pt–Ba/Al_2O_3 and Pt/Al_2O_3 catalysts. It is important to underline that the temperature has an important effect on both the NO_x storage capacity and the efficiency of the reducing agent. These two aspects influence the total amounts of the reduction products (being related to the NO_x stored amounts) and the selectivity of the process (i.e. the relative amounts of the same reduction products). As expected, by increasing the temperature the NO_x storage capacity increases as well [26], and the reducing agent becomes more efficient in the reduction [31]. Temperature also affects N_2O formation, as summarized in Fig. 6 showing the outlet N_2O concentration profiles and

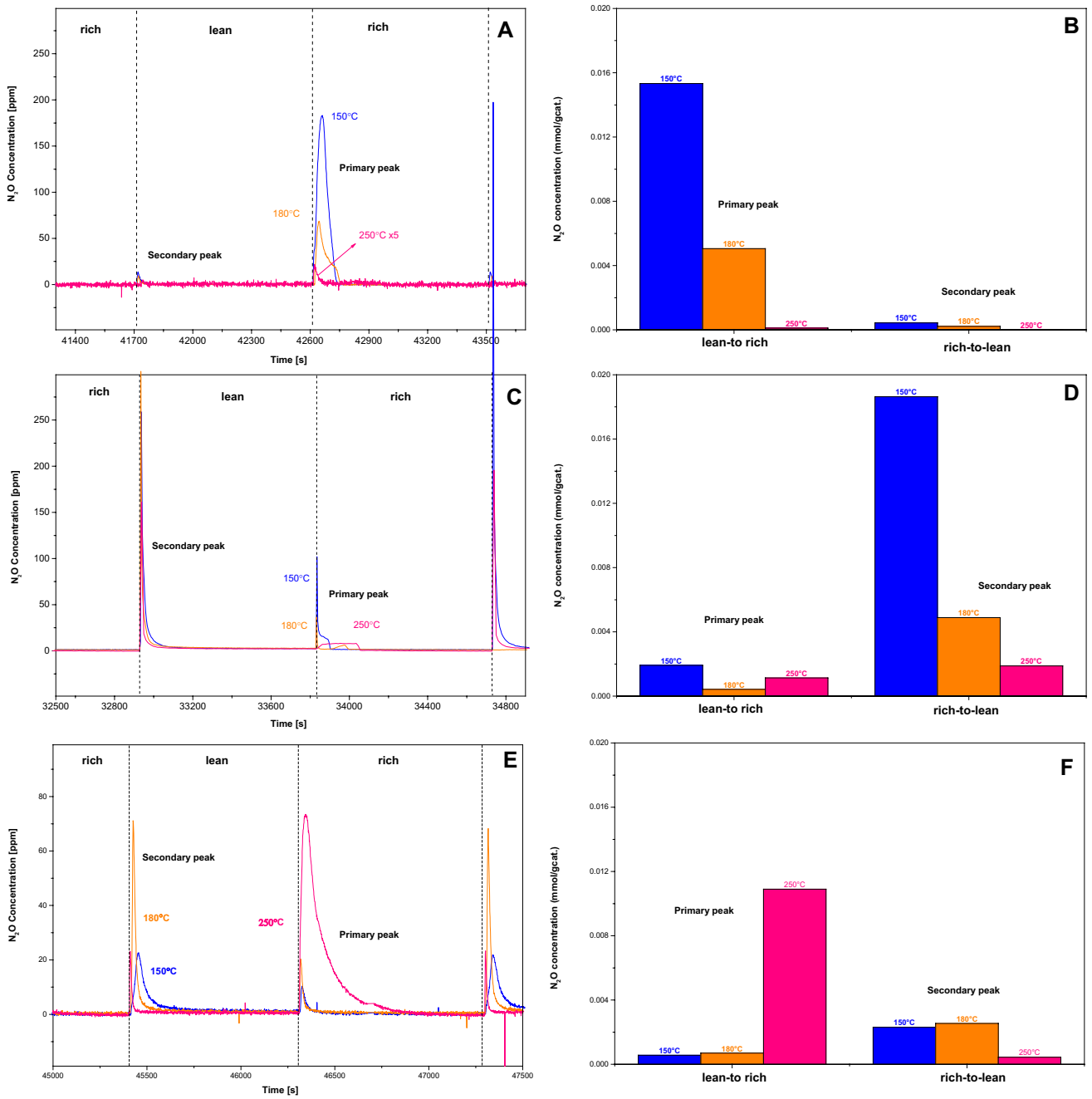

Fig. 6 N_2O profile during lean-rich cycles at different temperature (e.g. 150, 180, 250 °C) over **a, b** Pt–Ba/Al_2O_3 catalyst, using H_2 as reductant; **c, d** Pt/Al_2O_3 catalyst, using H_2 as reductant; **e, f** Pt–Ba/Al_2O_3 catalyst, using C_3H_6 as reductant

the amounts of N_2O emitted at different temperatures in the case of Pt–Ba/Al_2O_3 when using H_2 (Fig. 6a, b) or propylene (Fig. 6e, f) as reductants, and in the case of the Pt/Al_2O_3 (Fig. 6c, d) catalyst (H_2 reductant).

In the case of Pt–Ba/Al_2O_3, when H_2 is used as reductant the primary N_2O formation is higher than the secondary at all the investigated temperatures (see Fig. 6a, b); temperature strongly decreases both the primary and secondary the N_2O formation. In the case of primary N_2O emissions (lean-to-rich transition), it has been suggested that N_2O is formed at the regeneration front, upon admission of the reductant (H_2) that leads to the release of gaseous NO upon decomposition of the stored NO_x. Evolved NO is then reduced over the platinum sites; at the beginning of the reduction phase, Pt sites are only partially reduced (they were in the oxidized state during the previous lean phase) and accordingly NO is reduced primarily to N_2O according to the following scheme:

$$NO + Pt \rightarrow Pt - NO \quad (1)$$

$$Pt - NO + Pt \rightarrow Pt - N + Pt - O \quad (2)$$

$$Pt - NO + Pt - N \rightarrow N_2O + 2Pt \quad (3)$$

As the reduction process goes on, Pt–O sites are more reduced by the reductant thus restoring Pt metal sites (reactions (4)–(5)):

$$H_2 + 2Pt \rightarrow 2Pt - H \quad (4)$$

$$2Pt - H + Pt - O \rightarrow 3Pt + H_2O \quad (5)$$

Over fully reduced metal sites, NO is readily decomposed to N- and O-adspecies; while O-adspecies are scavenged by H_2 leading to water (reaction (5)), N-adspecies lead to N_2 and NH_3 formation (reactions (6) and (7)):

$$2Pt - N \rightarrow 2Pt + N_2 \quad (6)$$

$$Pt - N + 3Pt - H \rightarrow 4Pt + NH_3 \quad (7)$$

It is therefore clear that the oxidation degree of the Pt metal sites and the relative surface concentrations of the N-, H-, and O-adsorbed entities are the main factors governing the reduction products distribution, and as consequence the selectivity of the reduction process [32].

Notably, the product selectivity measured at the reactor outlet (see Fig. 7a in the case of H_2) is affected by the development of a reduction front along the catalytic bed, due to the integral nature of the trap. In fact, according with the sequential mechanism already proposed in the literature [33, 34], the so-formed ammonia may further react with NO_x species stored downstream the front leading to the formation of N_2. This has been very well documented by reaction studies were ammonia has been used as reductant [18, 21, 34]. In this respect, the chance of N_2O to further react with some surface species is also of interest, and will be discussed later on.

At variance, over the investigated Pt–Ba/Al_2O_3 sample, secondary N_2O formation is very small, and is visible only at low temperature. It has been suggested that N_2O formation occurs in this case due to the reaction between NO/O_2 fed upon the lean phase and reductive species (like NCO, CO or NH_3) in an adsorbed state, as reported also by Bártová et al. [5, 9]. In view of the significant NH_3 production observed in this case at low temperatures, it is very likely that part of the formed ammonia remains adsorbed on the surface (in small amounts due to the basicity of the surface) and this is responsible for the small N_2O peak observed upon the rich-to-lean transition.

Temperature strongly decreases both primary and secondary N_2O formation (see Fig. 6a) and pushes the selectivity to N_2 (Fig. 7a). In the case of the primary N_2O formation, this is related to the fast reduction of the Pt sites that accordingly efficiently decompose NO to N- and O-adspecies, thus favoring N_2, NH_3 and H_2O formation through reactions (1), (2), (4), (5) and (7). Along similar lines, secondary N_2O formation decreases with temperature due to the decrease of the adsorbed ammonia.

In the case of Pt/Al_2O_3 (Fig. 6c, d), primary N_2O formation is much smaller due to the lower amounts of stored NO_x and hence due to the decrease of gas-phase NO concentration released upon the rich phase. At variance, the secondary N_2O peak, originated at the rich-to-lean transition, is higher than the primary one and it is much higher that observed in the case of the Pt–Ba/Al_2O_3 sample. As pointed out by FTIR measurements, in the case of Pt/Al_2O_3 catalyst at the end of the rich phase some ammonia is still present at the catalyst surface (Fig. 4b). This ammonia can react with gaseous NO/O_2 fed at the beginning of the lean phase, giving N_2O, in line with the well-known selectivity to nitrous oxide of the NH_3+NO reaction in the presence of O_2 over PGM-based catalysts [35]. The higher amounts of adsorbed ammonia with respect to Pt–Ba/Al_2O_3 are in line with the higher acidity of the Pt/Al_2O_3 sample. Again, also in this case temperature increase decreases secondary N_2O formation due to the decrease of the amounts of ammonia stored on the catalyst surface.

Finally, in the case of Pt–Ba/Al_2O_3 (Fig. 6e, f) when propylene is used as reductant, a more complex picture is observed since primary N_2O formation increases with temperature in the investigated T-range, whereas the opposite is seen for secondary N_2O formation. The increase with temperature of the primary N_2O formation is related to the increase in the amounts of stored NO_x and to the poor reactivity of propylene as reductant. In fact, in this case even at 250 °C the reduction of the Pt sites proceeds rather slowly and accordingly significant amounts of N_2O could be formed. At variance, concerning secondary N_2O formation, as apparent from Fig. 8 isocyanates species and CO adsorbed on Pt sites are well detected by FT-IR. Indeed, as it appears in Fig. 8 for the rich phase at 250 °C, bands characteristic of CO adsorbed on Pt (band at 2067 cm^{-1} which shifts towards 2050 cm^{-1}) and of isocyanates NCO^- on Ba sites (band at 2170 cm^{-1}) rapidly grow up showing a maximum after 2 min and an intensity loss for higher contact time [31], a typical behavior of intermediate species. CO is formed during the reduction of stored NO_x with C_3H_6 according to a reforming reaction; the so-formed CO then reacts with adsorbed NO_x leading to adsorbed isocyanates species, that remain onto the catalytic surface at the end of the rich phase. At the rich-to-lean switch NCO species could react with NO/O_2 leading to secondary N_2O formation.

3.2 N_2O Reactivity

In order to check whether N_2O is a terminal species or it may be involved in subsequent reactions once formed, the

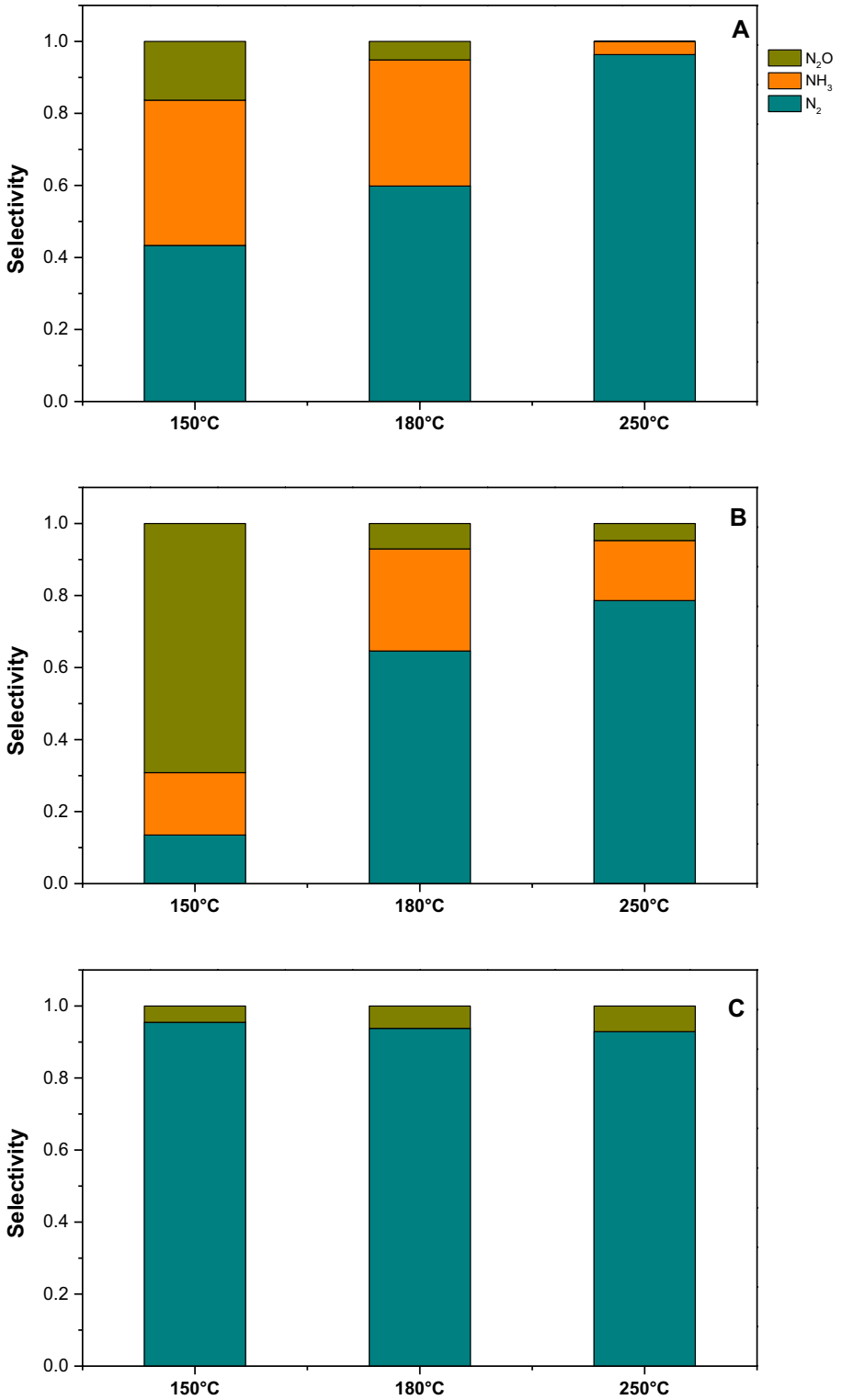

Fig. 7 Selectivity of the reduction phase at different temperature (e.g. 150, 180, 250 °C) over **a** Pt–Ba/Al_2O_3 catalyst, using H_2 as reductant; **b** Pt/Al_2O_3 catalyst, using H_2 as reductant; **c** Pt–Ba/Al_2O_3 catalyst, using C_3H_6 as reductant

reactivity on N_2O alone (N_2O decomposition) or using different reductants (N_2O reduction) has been investigated over Pt–Ba/Al_2O_3 and Pt/Al_2O_3 catalysts. The results of the decomposition studies, carried out upon heating the samples from room temperature up to 500 °C are shown in Fig. 9a, b in the case of Pt–Ba/Al_2O_3 and Pt/Al_2O_3, respectively. The onset temperature for N_2O decomposition in both cases is near 400 °C; at 500 °C (maximum ramp temperature) the N_2O conversion is near 30%. N_2O decomposition leads to the production of N_2 and O_2. As shown by the figures, the

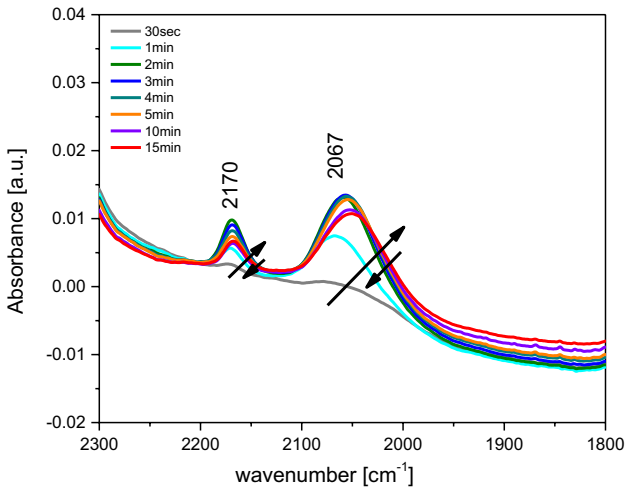

Fig. 8 *Operando* FT-IR spectra at 250 °C over Pt–Ba/Al_2O_3 catalyst during the rich phase in C_3H_6 450 ppm + 0.5% v/v H_2O in He

reactivity of N_2O in the decomposition reaction is very poor, and therefore does not occur in the investigated temperature range of lean-rich cycles.

The reactivity of N_2O towards different reducing agent (H_2, NH_3, C_3H_6) has also been studied over both Pt–Ba/Al_2O_3 and Pt/Al_2O_3, and results are compared in Fig. 10 in terms of N_2O concentration. H_2 and C_3H_6 have been considered being the actual reducing agents investigated in this work; the reactivity of ammonia has also been investigated being NH_3 formed upon reaction of the stored NO_x with H_2.

In the case of H_2, over the ternary system the reduction of N_2O starts near 90 °C (Fig. 10a) leading to the formation of N_2 only (not shown). A slightly lower temperature is observed in the case of the binary system (i.e. near 80 °C, Fig. 10b). However, whereas N_2O consumption is complete below 250 °C in the case of the Pt–Ba/Al_2O_3 sample, over the Ba-free sample complete consumption of N_2O is attained slightly below 300 °C. This indicates that the presence of Ba slightly increase the catalyst reactivity.

There is now a general consensus on the fact that the N_2O decomposition/reduction over noble metal catalysts involves the formation of O-adspecies (reactions (8), (9)) [10 and ref herein reported]; in the absence of reducing agents, the rate determining step is the recombination of the oxygen adsorbed species with release of molecular oxygen (reaction (11)):

$$N_2O + * \rightarrow N_2O * \quad (8)$$

$$N_2O * \rightarrow N_2 + O * \quad (9)$$

$$N_2O + O * \rightarrow N_2 + O_2 + * \quad (10)$$

$$2O * \rightarrow O_2 + 2 * \quad (11)$$

As shown in Fig. 9, this process likely occurs only at high temperatures, being the decomposition of N_2O observed only above 300 °C.

At variance, in the presence of a reductant (H_2), adsorbed oxygen species are scavenged by H_2 and the reaction proceeds at much low temperatures (reaction 12):

$$O * + H_2 \rightarrow H_2O + * \quad (12)$$

Since the rate determining step for the N_2O reduction is the removal of surface oxygen, the efficiency of N_2O reduction/decomposition depends on the capacity of the reductants and/or the catalyst to facilitate these reactions.

This reaction scheme is supported by several authors. In particular, Cant et al. [36] have demonstrate that the reduction of $^{15}N^{14}NO$ by hydrogen over a Rh/SiO_2 catalyst yields $^{15}N^{14}N$ as the exclusive nitrogen-containing product. This result rules out a suggestion in the literature that the reduction proceeds through cleavage of the N–N bond. Moreover, McCabe et al. [37] report that the reaction orders and apparent activation energy are consistent with a mechanism involving reaction between adsorbed reductant (in that case CO) and adsorbed N_2O dissociation products.

Figure 10 previously discussed in the case of H_2 as reducing agent points out that N_2O can be reduced at low temperatures by H_2. This may suggest that there is a chance, at the regeneration front, for the forming (native) N_2O to be at least partially reduced by H_2. However downstream the regeneration front, i.e. in the absence of gaseous H_2, N_2O does not react with the catalyst surface.

Figure 10a, b also compares the N_2O concentration profiles measured during the reduction with the different reducing agents as function of temperature over Pt–Ba/Al_2O_3 and Pt/Al_2O_3, respectively.

Comparing the onset temperature for N_2O consumption the following order of reactivity is apparent: $H_2 \sim NH_3 > C_3H_6$. The same reactivity order is observed in the case of Pt–Ba/Al_2O_3 and Pt/Al_2O_3, although on the Ba-free sample ammonia reacts faster than hydrogen even if its onset temperature is higher.

As already discussed in the case of hydrogen, the main role of the reducing agent is to remove adsorbed oxygen species from the surface allowing the N_2O reduction. O_2 species are scavenged by ammonia and propylene according to the following overall reactions:

$$3O * + 2NH_3 \rightarrow N_2 + 3H_2O + 3 * \quad (13)$$

$$9O * + C_3H_6 \rightarrow 3CO_2 + 3H_2O + 9 * \quad (14)$$

Since propylene exhibits a lower capacity than hydrogen and ammonia to promote these reactions, the onset temperature of N_2O consumption is observed at higher temperatures.

Interestingly, the temperature range where ammonia is able to convert N_2O is the same where N_2O evolution is

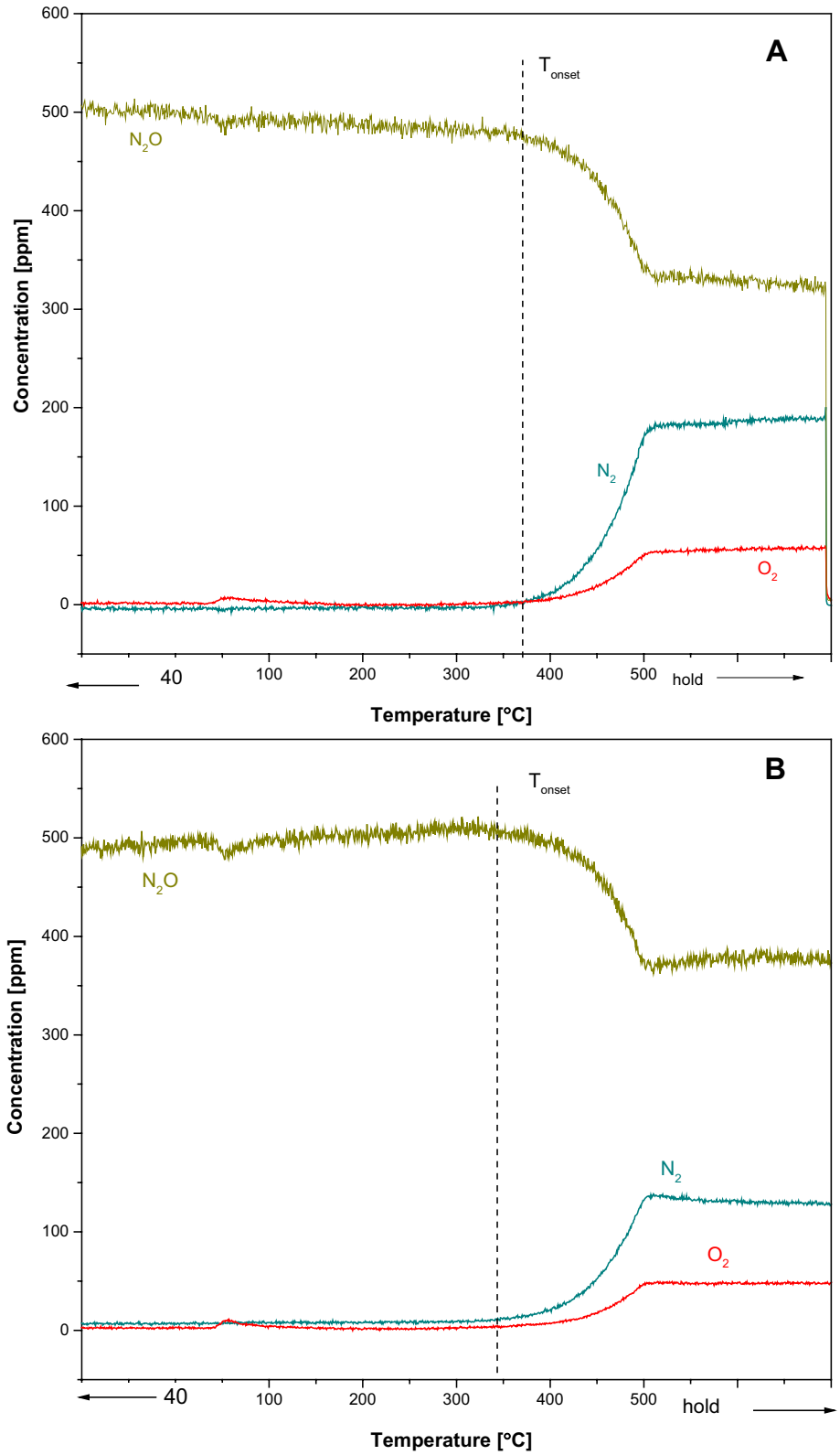

Fig. 9 N_2O thermal decomposition in He in the presence of CO_2 (1000 ppm) + H_2O (2.5%) over **a** Pt–Ba/Al_2O_3 and **b** Pt/Al_2O_3 catalysts. Heating ramp: from room temperature to 500, 10 °C/min

seen during the experiments. Since ammonia, like N_2O, is formed at the regeneration front and travels along the catalyst bed, there is a chance for this species to decrease N_2O concentration. However, since ammonia also reacts with NO_x stored downstream the H_2 regeneration front at such temperatures, very likely its efficiency in the N_2O

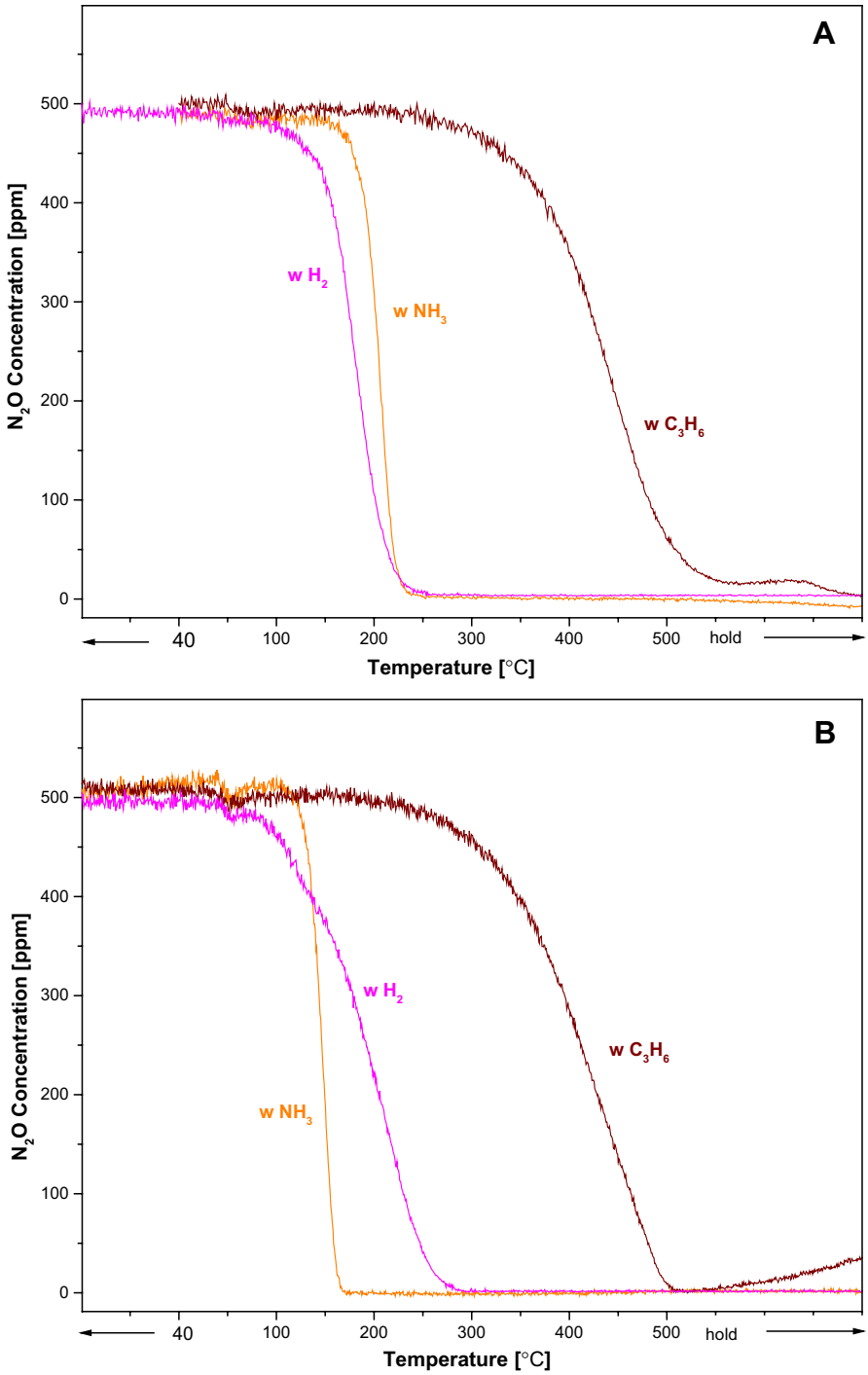

Fig. 10 N_2O reduction in the presence of CO_2 (1000 ppm) + H_2O (2.5%) over **a** Pt–Ba/Al_2O_3 and **b** Pt/Al_2O_3 catalysts. Reductant concentrations: H_2 (2000 ppm), NH_3 (1000 ppm), C_3H_6 (1000 ppm); heating ramp: from room temperature to 500, 10 °C/min

reduction is limited, although a role of ammonia in the decrease of N_2O emissions cannot be ruled out.

4 Concluding Remarks

In this paper, mechanistic aspects involved in the formation and reduction of N_2O over a model Pt–Ba/Al_2O_3 LNT catalyst have been investigated by means of simultaneous gas phase and surface analysis using FT-IR spectroscopy. N_2O evolution is observed both at the lean-to-rich (primary N_2O) and rich-to-lean (secondary N_2O) switches. In particular, when hydrogen is used as reductant: (i) primary N_2O formation is significant, secondary N_2O is negligible; (ii) without the supported Ba phase (Pt–Al_2O_3 sample), also secondary N_2O is significant and higher with respect to the primary one; (iii) without the Ba phase, surface intermediate species, i.e. ammonia and ammonium ions, not present in the case of

Pt–Ba/Al_2O_3, are detected; (iv) in all cases, the production of both primary and secondary N_2O decreases on increasing temperature. Moreover, when a poor reductant like propylene is used, also in the case of Pt–Ba/Al_2O_3 the secondary N_2O production is higher than the primary one and surface intermediate species, i.e. isocyanates and CO adsorbed on Pt sites, are well detected by FT-IR.

All these results suggest that primary N_2O is formed when undissociated NO in the gas phase and partially reduced metal sites are present, while secondary N_2O originates from reaction between surface intermediate species and residual NO_x at the beginning of the lean phase.

The reactivity of N_2O towards different reducing agent (H_2, NH_3, C_3H_6) has been studied under programming temperature (TPR). Comparing the onset temperature of N_2O consumption, it appears that, as expected, stronger is the reductant lower is the onset temperature; their reactivity order is the same for Pt–Ba/Al_2O_3 and Pt/Al_2O_3 catalyst, that is: $H_2 \sim NH_3 > CO > C_3H_6$. The reduction is completely selective to nitrogen and occurs at temperature higher than 250 °C in the case of Pt–Ba/Al_2O_3 catalyst, while lower temperatures are detected for Pt/Al_2O_3 catalyst. The rate determining step for deN_2O is the removal of surface oxygen; as a consequence, the efficiency of N_2O reduction/decomposition depends on the capacity of the reductants and/or the catalyst to facilitate these reactions. Considering that H_2 has a high reactivity in the reduction of N_2O, it may reacts with N_2O that is forming at the regeneration front. Moreover, also ammonia present downstream to the H_2 front has the chance to reduce N_2O, although this species is more likely involved in the reaction with NO_x stored downstream the H_2 front.

References

1. Bielaczyc P, Woodburn J, Szczotka A (2014) Appl Energy 117:134–141
2. Chen Y, Borken-Kleefeld J (2014) Atmos Environ 88:157–164
3. Lietti L, Daturi M, Blasin-Aubé V, Ghiotti G, Prinetto F, Forzatti P (2012) ChemCatChem 4(1):55–58
4. Lashof DA, Ahuja DR (1990) Nature 344(6266):529
5. Bártová Š, Kočí P, Mráček D, Marek M, Pihl JA, Choi J-S, Toops TJ, Partridge WP (2014) Catal Today 231:145–154
6. Choi J-S, Partridge WP, Pihl JA, Kim M-Y, Kočí P, Daw CS (2012) Catal Today 184(1):20–26
7. Clayton RD, Harold MP, Balakotaiah V (2009) AIChE J 55(3):687–700
8. Dasari P, Muncrief R, Harold MP (2013) Top Catal 56(18):1922–1936
9. Kočí P, Bártová Š, Mráček D, Marek M, Choi J-S, Kim M-Y, Pihl JA, Partridge WP (2013) Top Catal 56(1):118–124
10. Jabłońska M, Palkovits R (2016) Catal Sci Technol 6:7671–7687
11. Ohnishi C, Asano K, Iwamoto S, Chikama K, Inoue M (2007) Catal Today 120:145–150
12. Xue L, He H, Liu C, Zhang C, Zhang B (2009) Environ Sci Technol 43:890–895
13. Grzybek G, Stelmachowski P, Gudyka S, Indyka P, Sojka Z, Guillén-Hurtado N, Rico-Pérez V, Bueno-López A, Kotarba A (2016) Appl Catal B 180:622–629
14. Zou W, Xie P, Hua W, Wang Y, Kong D, Yue Y, Ma Z, Yang W, Gao Z (2014) J Mol Catal A 394:83–88
15. Zhang X, Shen Q, He C, Ma C, Cheng J, Liu Z, Hao Z (2012) Catal Sci Technol 2:1249–1258
16. Piumetti M, Hussain M, Fino D, Russo N (2015) Appl Catal B 165:158–168
17. Kim SS, Lee SJ, Hong SC (2011) Chem Eng J 169:173–179
18. Cumaranatunge L, Mulla SS, Yezerets A, Currier NW, Delgass WN, Ribeiro FH (2007) J Catal 246(1):29–34
19. Tamm S, Andonova S, Olsson L (2014) Catal Lett 144(7):1101–1112
20. Nova I, Lietti L, Castoldi L, Tronconi E, Forzatti P (2006) J Catal 239(1):244–254
21. Partridge WP, Choi J-S (2009) Appl Catal B 91(1):144–151
22. Forzatti P, Lietti L, Castoldi L (2015) Catal Lett 145(2):483–504
23. Castoldi L, Righini L, Matarrese R, Lietti L, Forzatti P (2015) J Catal 328:270–279
24. Castoldi L, Matarrese R, Morandi S, Righini L, Lietti L (2018) Appl Catal B 224:249–263
25. Lietti L, Forzatti P, Nova I, Tronconi E (2001) J Catal 204:175–191
26. Morandi S, Prinetto F, Ghiotti G, Castoldi L, Lietti L, Forzatti P, Daturi M, Blasin-Aubé V (2014) Catal Today 231:116–124
27. Centi G, Perathoner S, Biglino D, Giamello E (1995) J Catal 152:75–92
28. Ramis G, Larrubia MA (2004) J Mol Catal A 215:161–167
29. Sobczyk DP, Hesen JJG, van Grondelle J, Schuring D, de Jong AM, van Santen RA (2004) Catal Lett 94:37–43
30. Righini L, Kubiak L, Morandi S, Castoldi L, Lietti L, Forzatti P (2014) ACS Catal 4:3261–3272
31. Castoldi L, Matarrese R, Kubiak L, Daturi M, Artioli N, Pompa S, Lietti L (2018) Catal Today. https://doi.org/10.1016/j.cattod.2018.01.026 (**in press**)
32. Lietti L, Artioli N, Righini L, Castoldi L, Forzatti P (2012) Ind Eng Chem Res 51:7597–7605
33. Bhatia D, Clayton RD, Harold MP, Balakotaiah V (2009) Catal Today 147S:S250
34. Lietti L, Nova I, Forzatti P (2008) J Catal 257:270
35. Scheuer A, Hauptmann W, Drochner A, Gieshoff J, Vogel H, Votsmeier M (2012) Appl Catal B 111:445–455
36. Cant NW, Chambers DC, Liu IO (2011) J Catal 278:162–166
37. McCabe RW, Wong C (1990) J Catal 121:422–431